Characterization of Spontaneously Arising Chlorhexidine-Tolerant Variants in *Streptococcus mutans*

Justin R. Kaspar[1#], Matthew J. Godwin[1], Irina M. Velsko[2,3],
Vincent P. Richards[2], and Robert A. Burne[1]

[1]Department of Oral Biology, University of Florida, Gainesville, Florida
[2]Department of Biological Sciences, Clemson University, Clemson, South Carolina
[3]Max Planck Institute for the Science of Human History, Jena, Germany

[#] Corresponding author
Mailing address: Department of Oral Biology, University of Florida, College of Dentistry,
P.O. Box 100424, Gainesville, FL 32610.
Phone: (352) 273-8848
E-mail: jkaspar@dental.ufl.edu
Twitter: @jkaspar11 , @BurneLabUF , @UFBiol

Running title: chlorhexidine-tolerant variants of *Streptococcus mutans*

Keywords: dental caries, *Streptococcus mutans*, oral microbiome, antimicrobials, antimicrobial tolerance, chlorhexidine, biofilms, microbial antagonism, stress response

ABSTRACT

Broad spectrum antimicrobials, both in dental products and within the clinic, have been used in the suppression of cariogenic bacteria such as *Streptococcus mutans* for over 40 years. One such antimicrobial is chlorhexidine (CHX), and serves as a standard in dental research against which other antimicrobial therapies are compared against for their efficacy. However, very little is known about the mode of action for CHX against Streptococci and whether tolerance can be developed from repeated exposures. Here, we begin to answer such questions by passaging *S. mutans* with increasing concentrations of CHX and isolating spontaneously-arising tolerant variants (CTVs) from separate lineages. We find that these CTVs display a higher minimal inhibitory concentration (MIC) against CHX than the wild-type strain and have altered virulence properties such as acid tolerance and biofilm formation. We record higher MICs for the variants against both daptomycin and bacitracin, but find increased sensitivity to triclosan and sodium fluoride. Measurements of antagonistic capabilities against other health-associated oral streptococci show decreased bacteriocin production compared to wild-type and increased sensitivity to hydrogen peroxide. Finally whole genome sequencing of the CTVs show common single nucleotide polymorphisms (SNPs) within a diacylglycerol kinase homolog and a glycolipid synthesis enzyme, altering LTA accumulation and potentially lipid profile of the cell wall. Together, these findings confirm that streptococci may develop tolerance to antimicrobial agents such as CHX but in the case of *S. mutans*, increased tolerance may come at a fitness cost for survival within oral biofilms that keeps variants suppressed within the population.

INTRODUCTION

Controlling microbial biofilm infections in humans is challenging in part due to the presence of extracellular polymeric substances (EPS) in which the organisms are embedded, the presence of persister cells and sub-populations of cells with low metabolic activity, and exchange of antimicrobial resistance genes through horizontal gene transfer. In the human oral cavity, accumulation of biofilms on the teeth can lead to destruction of tooth mineral when there is frequent and significant localized acidification by organic acids produced as metabolic end products from fermentable carbohydrates (1). The initiation and progression of dental caries can be controlled to a degree through non-specific mechanical removal of the biofilms or by treatment with various chemical agents that include fluoride, xylitol or chlorhexidine (CHX) (2, 3). While the effectiveness of CHX in caries prevention is not definitively established and there can be undesirable side effects (e.g. staining, irritation of host tissues) (4), CHX remains a standard against which antimicrobial therapies are compared for their efficacy in the suppression of caries-causing bacteria, such as *Streptococcus mutans* (5–7). Currently in the United States, mouth rinses containing 0.12% CHX are the only CHX-containing products marketed for caries prevention (4).

Chlorhexidine is a bisbiguanide agent and has diverse medical applications as a disinfectant for surfaces and as an antiseptic for topical applications. However, the mode of action of CHX is poorly understood. CHX, which is positively charged at neutral pH, is thought to be attracted to the bacterial cell surface, where it may electrostatically interact with negatively charged phospholipids (8). Depending on the concentration of CHX, it can reduce bacterial membrane fluidity or disrupt the structural integrity of the membrane(s), causing increased permeability, leakage of cell contents, and cell death. In one study (9), it was found that CHX induces the formation of dented spots on the surface of the cell wall of both *Escherichia coli* and *Bacillus subtilis*. The authors posited that the structural changes of the bacterial cell wall may be due to the action of CHX with membrane cardiolipin and phosphatidylethanolamine to disturb the normal arrangement and integrity of the phospholipid bilayer structure and its associated proteins (9).

While CHX likely puts substantial selective pressure on *S. mutans* and the oral microbiota in general, particularly if used repeatedly for oral care, the organisms appear to

remain susceptible to CHX, with few reports of resistance (10). However one recent study (6) reported that when CHX was continuously flowed on biofilms formed on polystyrene blocks *in vitro*, detached cells displayed a higher minimal inhibitory concentration (MIC) to CHX (1.25 μg mL^{-1}), whereas most isolates of *S. mutans* evaluated had MICs < 1μg mL^{1}. In enterococci, increased tolerance to antiseptics such as CHX in the hospital setting has inspired research into methods of increased CHX tolerance, including studies of CHX effects on the transcriptome (11) and on a transposon mutant library (12). More specifically, Bhardwaj and colleagues (11) used RNA-Seq to show that VanA-type vancomycin resistance genes are upregulated in *Enterococcus faecium* following CHX exposure. In *E. faecium*, two genes encoding for a two-component regulatory system were found to contribute to CHX tolerance (12). Thus, it is clear that Firmicutes have the capacity to develop increased tolerance to CHX, however the mechanisms by which tolerance may develop, especially in streptococci, is only beginning to be explored.

In this study, we find that *S. mutans* passaged with increasing concentrations of CHX can acquire increased tolerance and/or resistance to CHX. We then characterized these chlorhexidine tolerant variants (CTVs) of *S. mutans* for their abilities to display critical virulence properties. Additionally, we demonstrate that CTVs also become more or less susceptible to a variety of other antimicrobials. Through whole genome sequencing, we survey the genomes of selected CTVs to identify SNPs that may contribute to CHX-tolerance. Data is also presented that spontaneously-arising CTVs may not be as prevalent in isolates of *S. mutans* because of adverse effects of the adaptation on the tolerance by the variants of antagonistic activities of commensal bacteria. Collectively, this study sheds light on the molecular basis for bacterial tolerance of CHX and the mechanisms of action of CHX that together may inform the development of more effective treatments for removal of cariogenic bacteria from oral biofilm communities.

RESULTS AND DISCUSSION

Selection for Chlorhexidine Tolerant Variants.

To determine how *S. mutans* may adapt to repeated CHX exposures over time, we initially determined the MIC for growth of *S. mutans* strain UA159. The wild-type strain was then passaged on BHI agar plates containing various concentrations of CHX **(Figure 1A)**. Colonies able to grow on the highest concentration CHX agar plate were picked, regrown in BHI broth under non-selective conditions, and then plated on a higher concentration of CHX. The selections were then repeated with one additional round using higher concentrations of CHX and the colonies were stored for further analysis. To acquire the first generation of spontaneously-arising CHX tolerant *S. mutans* variants (CTVs), $1x10^6$ CFUs of *S. mutans* grown in BHI broth to $OD_{600\ nm}$ = 0.5 (mid-exponential log phase) was spread on BHI agar plates containing 0.1, 0.25 or 0.5 μg mL^{-1} CHX. While the plates containing 0.1 or 0.25 μg mL^{-1} CHX yielded lawns of bacteria, individual colonies were obtained on the 0.5 μg mL^{-1} agar plates, consistent with a prior report on the MIC of CHX for *S. mutans* (10). No colonies could be obtained in the first round of plating on BHI agar plates supplemented with 0.75 μg mL^{-1} CHX. Ten individual bacterial colonies were selected from the 0.5 μg mL^{-1} plate, designated as CTV1s (CHX tolerant variants from the 1st generation) and grown overnight in BHI broth. Cultures were diluted and regrown to $OD_{600\ nm}$ = 0.5, diluted to $1x10^6$ CFUs and 0.1 ml of each of the 10 individual CTV1 cultures were spread on BHI agar plates containing either 0.75, 1.0 or 1.25 μg mL^{-1} CHX, establishing 10 independent lineages moving forward to the second generation. Individual colonies were obtained on plates with all three concentrations of CHX. One colony was selected from each of the 1.25 μg mL^{-1} CHX plates to move forward to the third generation. After growth to $OD_{600\ nm}$ = 0.5 and dilution to $1x10^6$ CFUs, these 10 CTV2s were then plated on 1.5, 1.625 or 1.75 μg mL^{-1} CHX. Again, colonies were obtained on all concentrations. At this

point, one colony was selected from each of the CTV3 plates (1.75 μg mL^{-1} CHX) and stored for further analysis. Confirmation that the variants were indeed *S. mutans* was obtained by amplifying and sequencings 1.5 kbp of the 16S rDNA sequence from these ten CTV3s. Seven selected CTV3 *S. mutans* were subjected to further analysis.

To confirm that the selected seven CTV3s had elevated tolerance to CHX, an MIC test was conducted **(Figure 1B)**. All CTV3s were grown to OD_{600} = 0.5, then diluted 1/100 into the wells of a 96-well microtiter plate containing various concentrations of CHX. The plates were incubated for 24 h. While the parental strain UA159 could only grow in BHI broth containing 0.5 μg mL^{-1} CHX, all CTV3s were able to grow in BHI containing >0.5 μg mL^{-1} CHX. Interestingly, all seven CTV3s tested displayed different MICs, with the most tolerant isolate, CTV3-6, able to grow in BHI broth containing 1.25 μg mL^{-1} CHX. Other isolates, such as CTV3-1 and CTV3-8 were only able to grow in BHI broth containing 0.75 μg mL^{-1} CHX. These data indicated to us several important points. First, the seven selected CTV3s were diverse in that they were able to tolerate different levels of CHX, possibly indicative of the acquisition of different mutations. Second, none of the variants were able to grow at 1.75 μg mL^{-1} CHX in broth, although all could grow on BHI agar plates with that concentration of CHX. It is unclear why the cells were able to tolerate the incorporation of higher levels of CHX on plates, but we speculate that either CHX breakdown over the 48-h incubation period on plates was greater than during the 24-h incubation used for testing MICs in broth and/or components of agar could sequester or inactivate CHX. In any case, all isolates had greater MICs to CHX than UA159 and the observed differences in MICs between agar and broth are known to be dependent on assay conditions, the compound(s) tested and species of bacteria tested (13).

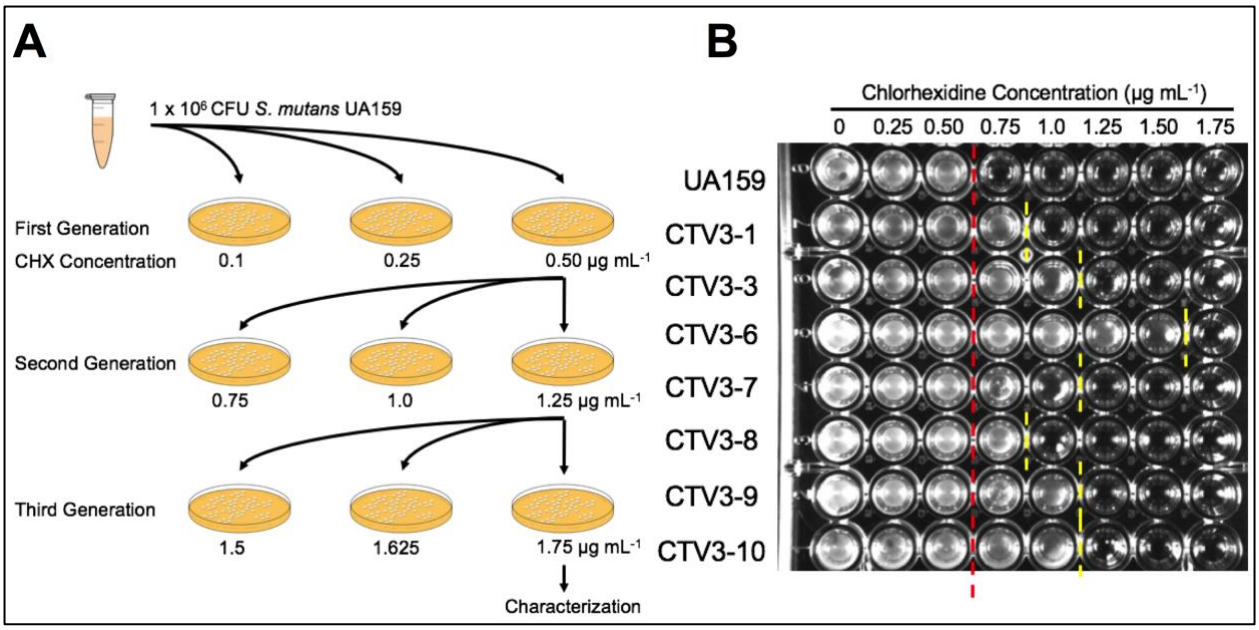

Figure 1. Acquisition of chlorhexidine tolerant variants. (A) Schematic of methods used to obtain the chlorhexidine tolerant variants (CTVs). ~1x10^{6} CFU of *S. mutans* UA159 grown to mid-exponential phase was spread plated on BHI agar plates containing either 0.1, 0.25 or 0.5 μg mL^{-1} CHX. Ten different single colonies were selected from the 0.5 μg mL^{-1} CHX plate to establish 10 independent lineages (CTV1). Cultures of these colonies were then plated on separate 0.75, 1.0 or 1.25 μg mL^{-1} CHX BHI agar plates (CTV2). One single colony from each plate was then cultured in BHI and plated on separate 1.5, 1.625 or 1.75 μg mL^{-1} CHX. At this point, one selected colony from each of the CTV3 plates was stored for further analysis and characterization. (B) Microtiter plate of the parental UA159 along with the CTV3s grown for 24 h in BHI with the designated concentrations of CHX. Red dotted line denotes highest concentration that the parental UA159 was able to grow and the yellow line denotes the highest concentration of growth for each of the CTV3s.

Attributes of the CTV3s.

We reasoned that mutations that rendered cells more tolerant of CHX could have pleiotropic effects, so several key properties of the variants were examined. We found that a majority of the CTV3s, except CTV3-1 and CTV3-9, had a shorter lag phase compared to the parental UA159 when diluted 1:100 dilution into fresh BHI broth. However, all CTV3s displayed slower exponential growth (i.e. longer doubling times) than the parental strain, ranging from 56 ± 2 min for CTV3-3 to 145 ± 26 min for CTV3-1, compared to 51 ± 2 for *S. mutans* UA159 **(Table 1)**. When growth rates in the presence of 0.75 μg mL^{-1} CHX were determined, the parental strain displayed little growth over a 24-h period (doubling time 623 ± 69 min, final yield 0.29 ± 0.09 $OD_{600\ nm}$), whereas all CTV3s displayed average doubling times under 150 min and final yields higher than 0.045 **(Figure 2B)**. Some variants, including CTV3-3, CTV3-8 and CTV 3-10, showed little difference in doubling times in the presence of absence of 0.75 μg mL^{-1} CHX. These data confirm that the selected CTV3s are more tolerant of CHX than the parental strain, and provide support for the idea that the disparate growth characteristics may reflect variation in the underlying genetic and physiologic bases for increased MICs to CHX.

One critical virulence attribute of *S. mutans* is acid tolerance (aciduricity), which allows organisms to continue metabolic processes at lower pH values than acid-sensitive oral organisms, leading to ecological shifts that promote caries development (14–16). Additionally, when *S. mutans* is cultured at acidic pH values, the fatty acid profile of the membrane is modified from mainly short-chained saturated fatty acids to a membrane with increased proportions of mono-unsaturated fatty acids with longer chains (17). Interestingly, all CTV3s had a shorter lag time when diluted from BHI into BHI that had been acidified with HCl to a pH of 5.5, compared to the parental UA159 **(Figure 2C)**. However, the doubling time of the CTVs was comparable to that of UA159, and UA159 had the highest final yield, as measured by optical density. When 0.75 µg mL^{-1} CHX was included in the acidified broth, UA159 failed to grow after 48 hours, while all CTV3s displayed growth **(Figure 2D)**. Some of the variants, including CTV3-3 and CTV3-7, actually displayed shorter doubling times and higher final yields when grown with CHX, compared with BHI at pH 5.5 with no added CHX. One possible explanation is that the variants have changes in the the phospholipid profile that allows them to be more toleratant of, and/or more rapidly adapt to, the low pH challenge.

The ability of the CTVs to compete with the parental strain and to form biofilms was also assessed. For competitive index measurements, a marked parental UA159 that included integration of an antibiotic resistance marker from pMC340B, which allow for single copy integration of a kanamycin resistance marker in the *mtlA* – *phnA* locus (18), was competed against unmarked UA159 and the CTV3s **(Figure 2E)**. In planktonic cultures, CTV3-3 and CTV3-10 were more competitive against UA159, whereas CTV3-9 was less competitive. These differences are consistent with the different growth rates displayed by UA159 and these CTV3s. In terms of biofilm formation, very little difference was observed in the biofilm biomass that formed in the chemically defined medium FMC with 20 mM glucose **(Figure 2F)**. However, with 15 mM glucose and 2.5 mM sucrose, CTV3-3, CTV3-6, CTV3-7 and CTV3-10 had impaired biofilm formation; accumulating 65-72% of the biomass attained by UA159, as measured by crystal violet staining. Conversely, CTV3-1 and CTV3-9 accumulated 170% and 270%, respectively, more biomass than UA159. How the acquired mutations and/or changes in gene regulation in the CTVs impact the biofilm phenotype will need to be further explored, but the differences observed in biofilm forming capacity futher highlights the diversity of the CTVs.

Table 1. Growth characteristics of CTV3s under different conditions.

Strain	Growth Characteristics							
	BHI pH 7.0		BHI pH 7.0 + 0.75 µg mL-1 CHX		BHI pH 5.5		BHI pH 5.5 + 0.75 µg mL-1 CHX	
	Doubling Time (min)	Final Yield (OD 600 nm)	Doubling Time (min)	Final Yield (OD 600 nm)	Doubling Time (min)	Final Yield (OD 600 nm)	Doubling Time (min)	Final Yield (OD 600 nm)
UA159	51 ± 2	0.61 ± 0.08	623 ± 69	0.29 ± 0.09	178 ± 12	0.65 ± 0.01	No growth	0.04 ± 0.02
CTV3-1	145 ± 26	0.45 ± 0.11	126 ± 19	0.41 ± 0.10	186 ± 11	0.45 ± 0.02	142 ± 14	0.23 ± 0.07
CTV3-3	56 ± 2	0.73 ± 0.14	78 ± 7	0.50 ± 0.04	259 ± 25	0.41 ± 0.01	142 ± 12	0.48 ± 0.02
CTV3-6	141 ± 16	0.55 ± 0.08	139 ± 17	0.44 ± 0.05	132 ± 14	0.32 ± 0.02	145 ± 8	0.31 ± 0.02
CTV3-7	108 ± 11	0.67 ± 0.05	143 ± 32	0.57 ± 0.11	142 ± 44	0.47 ± 0.02	119 ± 11	0.59 ± 0.09
CTV3-8	66 ± 7	0.72 ± 0.03	92 ± 13	0.59 ± 0.11	189 ± 34	0.54 ± 0.01	121 ± 12	0.59 ± 0.04
CTV3-9	97 ± 8	0.63 ± 0.04	133 ± 12	0.60 ± 0.01	160 ± 10	0.34 ± 0.01	215 ± 23	0.39 ± 0.11
CTV3-10	63 ± 6	0.56 ± 0.12	74 ± 5	0.52 ± 0.01	107 ± 7	0.55 ± 0.03	113 ± 22	0.59 ± 0.03

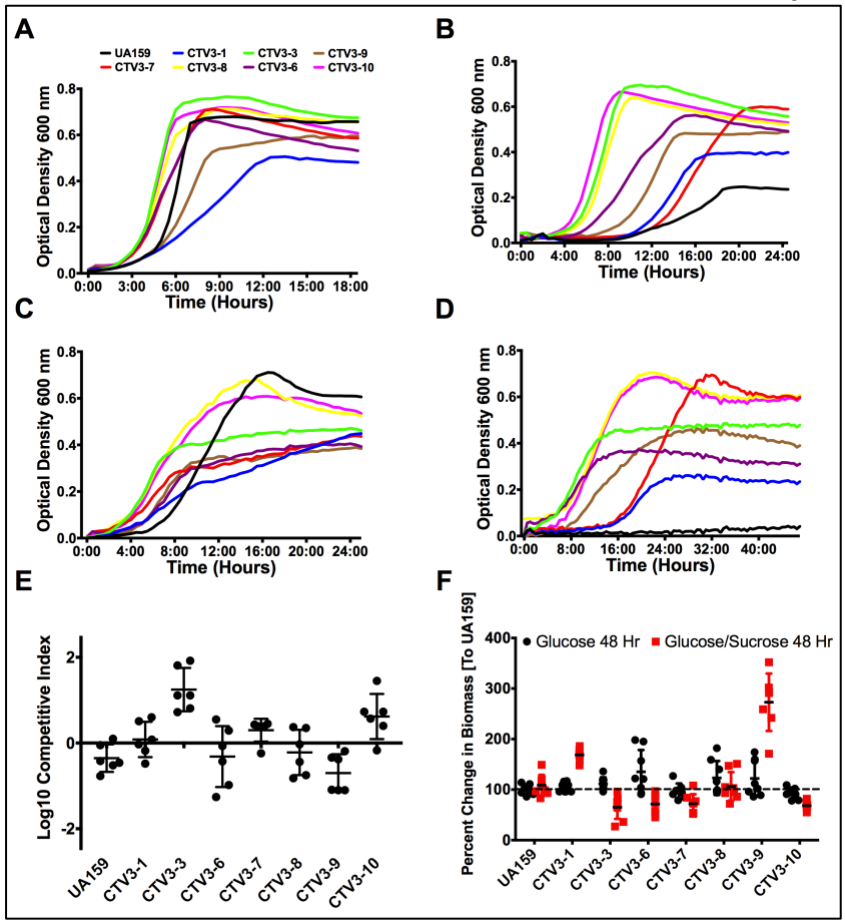

Figure 2. Growth attributes of the CTV3s. Growth of the parental UA159 strain (black line) and each of the CTV3s (colored lines) in either (A) BHI, (B) BHI with 0.75 µg mL^{-1} CHX, (C) BHI pH 5.5, and (D) BHI pH 5.5 with 0.75 µg mL^{-1} CHX. (E) Competitive index assay between the parental UA159 strain with the CTV3s in BHI medium after 24 h, competed with a marked parental UA159 that included integration of plasmid pMC340B (Km^{R}) that was used for selection. Data plotted is in the competitive index of the unmarked UA159 or the CTV3s. (F) Percentage change in biomass of biofilms grown for 48 hours in CDM medium supplemented with either 20 mM glucose (black dots) or 15 mM glucose and 2.5 mM sucrose (red dots) compared to the parental UA159, which was set to 100%.

CTV3s have reduced susceptibility to other antimicrobials.

Two recent studies with *E. faecium* and Methicillin-Resistant *Staphylococcus aureus* (MRSA) demonstrated reduced antibiotic susceptibility in strains that are less sensitive to CHX or the biguanide antiseptic polyhexanide, respectively (19, 20). To determine if a similar behavior was observable in our CTV3s, we determined MICs for the CTVs for six different antibiotics (amoxicillin, azithromycin, bacitracin, clindamycin, daptomycin, vancomycin) that

have different modes of action using the Etest Strip Assay **(Table 2)**. We saw no change in susceptibility to antibiotics that inhibit peptidoglycan cross-linking (amoxicillin, vancomycin), but drastic changes in bacitracin and daptomycin were evident **(Supplemental Figure 1)**. All variants, except for CTV3-9, displayed increased susceptibility to bacitracin, and all variants except for CTV3-1 showed higher MICs to daptomycin. The latter result is consistent with the fact that CHX and daptomycin target the cell wall (19, 20). Interestingly, the CTV3s showed reduced susceptibility to clindamycin, which inhibits protein synthesis through binding to the 50S ribosomal subunit (21), perhaps associated with decreased permeability or increased export of the drug in the CTV3s.

We next wanted to examine the susceptibility of the CTV3s to two compounds commonly used to prevent oral infectious diseases: triclosan and sodium fluoride. Triclosan is a broad-spectrum antibacterial, but unlike CHX, triclosan is more compatible with other ingredients commonly used in toothpastes. Triclosan also does not stain teeth or have an unpleasant taste, as does CHX, although CHX appears to have a more potent antibacterial properties (22). No observable growth differences were seen when the CTV3s were grown with 8 μg mL^{-1} triclosan **(Figure 3A)**, but when grown with 16 μg mL^{-1} triclosan all CTV3s grew more poorly than strain UA159 **(Figure 3B)**. Only variants CTV3-3, CTV3-8 and CTV3-10 displayed final yields similar to UA159, all others did not reach as high a final optical density. Fluoride is widely used in toothpastes and mouthwashes, and is typically added to municipal drinking water. Fluoride can not only arrest the demineralization of the tooth enamel, but at high concentrations (13 – 647 mM) it inhibits growth and metabolism of *S. mutans* (23, 24). Growth of the CTV3s compared to UA159 was slightly impaired with addition of 100 μg mL^{-1} sodium fluoride **(Figure 3C)**, but significant growth deficiencies were observed with 300 μg mL^{-1} sodium fluoride. Collectively, these observations show that the CTV3s may be more resistant to certain antibiotics, but they display increased sensitivity to agents that are commonly used in oral health formulations.

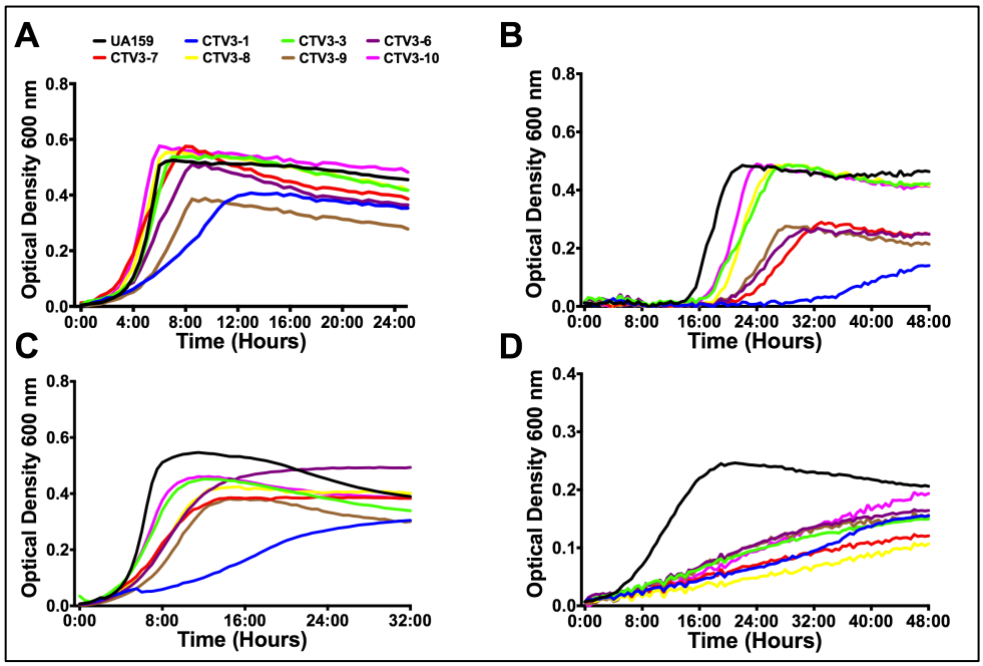

Figure 3. Changes in susceptibility to clinically-relevant antimicrobials. Growth of the parental UA159 strain (black line) and each of the CTV3s (colored lines) in either (A) 8 μg mL^{-1} triclosan, (B) 16 μg mL^{-1} triclosan, (C) 100 μg mL^{-1} sodium fluoride and (D) 300 μg mL^{-1} sodium fluoride.

Table 2. Changes in antibiotic sensitivity for CTV3s.

Antibiotic	Mechanism of Action	MIC Determined by ETest® Strips (μg mL^{-1})							
		UA159	CTV3-1	CTV3-3	CTV3-6	CTV3-7	CTV3-8	CTV3-9	CTV3-10
Amoxicillin	Inhibition of peptidoglycan cross-linkage	0.094	0.047	0.094	0.094	0.064	0.094	0.094	0.094
Azithromycin	Inhibition of protein synthesis	3	3	4	1.5	3	4	4	4
Bacitracin	Interference of peptidoglycan precursor transport to cell wall	128	48	64	96	96	96	192	96
Clindamycin	Inhibition of protein synthesis	0.064	0.125	0.094	0.125	0.094	0.125	0.19	0.125
Daptomycin	Insertion into cell membrane; loss of membrane potential	2	1.5	3	4	4	3	12	3
Vancomycin	Inhibition of peptidoglycan cross-linkage	1.5	1	1.5	1.5	1.5	1.5	1.5	1.5

CTV3s are Less Competitive Against Commensal Oral Streptococci.

As noted above (6), there is potential for spontaneously-arising variants that show decreased susceptibility to CHX that are selected within *S. mutans* populations *in vitro*, but such isolates have not been recovered from dental plaque. One possibility is that there are selective pressures imposed by host factors and the oral microbiota that keep spontaneously CHX-tolerant variants of *S. mutans* from developing in the human oral cavity.

To explore this idea, we investigated the antagonistic interactions of our CTV3s with species of commensal streptococci that are generally abundant and associated with dental health in humans. We measured bacteriocin production by our CTV3s using a deferred antagonism assay in which strains of *S. mutans* are stabbed on agar plates, grown overnight, and then the plates are overlaid with soft agar containing 10^7 cells of a sensitive indicator strain; in this case either *Streptococcus sanguinis* SK150 or *Streptococcus gordonii* DL1. Bacteriocin production was assessed by measuring the zones of growth inhibition of the indicator strain. When overlaid with *S. sanguinis* SK150, we found that the CTV3s displayed different-sized zones of inhibition, but that all were smaller than the parental UA159, indicating less bacteriocin production **(Figures 4A and 4C**). An even greater difference was observed when *S. gordonii* DL1 was used as the indicator strain, again with all CTV3s showing smaller zones of inhibition **(Figure 4B and 4D)**. We also performed a plate-based competition assay where *S. sanguinis* SK150 and our CTV3s were spotted next to each other at the same time and grown for 48 h **(Figure 4E)**. Whereas no zone of inhibition was seen when *S. sanguinis* SK150 and the parental UA159 were grown adjacent to one another, zones of inhibition where observed in all but two of the CTV3s, CTV3-1 and CTV3-8, indicating that the CTV3s did not compete as well as the parental. The simplest interpretation is that CTV3s produce less bacteriocins, decreasing their antagonistic capability towards other streptococci present in oral biofilms, and that their ability to tolerate hydrogen peroxide and possibly other antagonistic factors produced by commensal oral streptococci (25, 26) is concurrently diminished. To determine if CTV3s had marked differences in their sensitivity to H_2O_2 that could impact their fitness, the strains were cultured in BHI supplemented with H_2O_2. While differences were not observed in growth when 0.001% H_2O_2 was used **(Figure 4F)**, all CTV3s displayed decreased growth rates, compared to UA159, when challenged with 0.003% H_2O_2 **(Figure 4G)**. Thus, the spontaneous mutations that confer enhanced tolerance of CHX come at a cost to the competitive fitness of *S. mutans* in the form of decreased bacteriocin production and increased H_2O_2 susceptibility, which may account, at least in part, for the absence of CHX resistance among *S. mutans* isolates from human dental plaque samples.

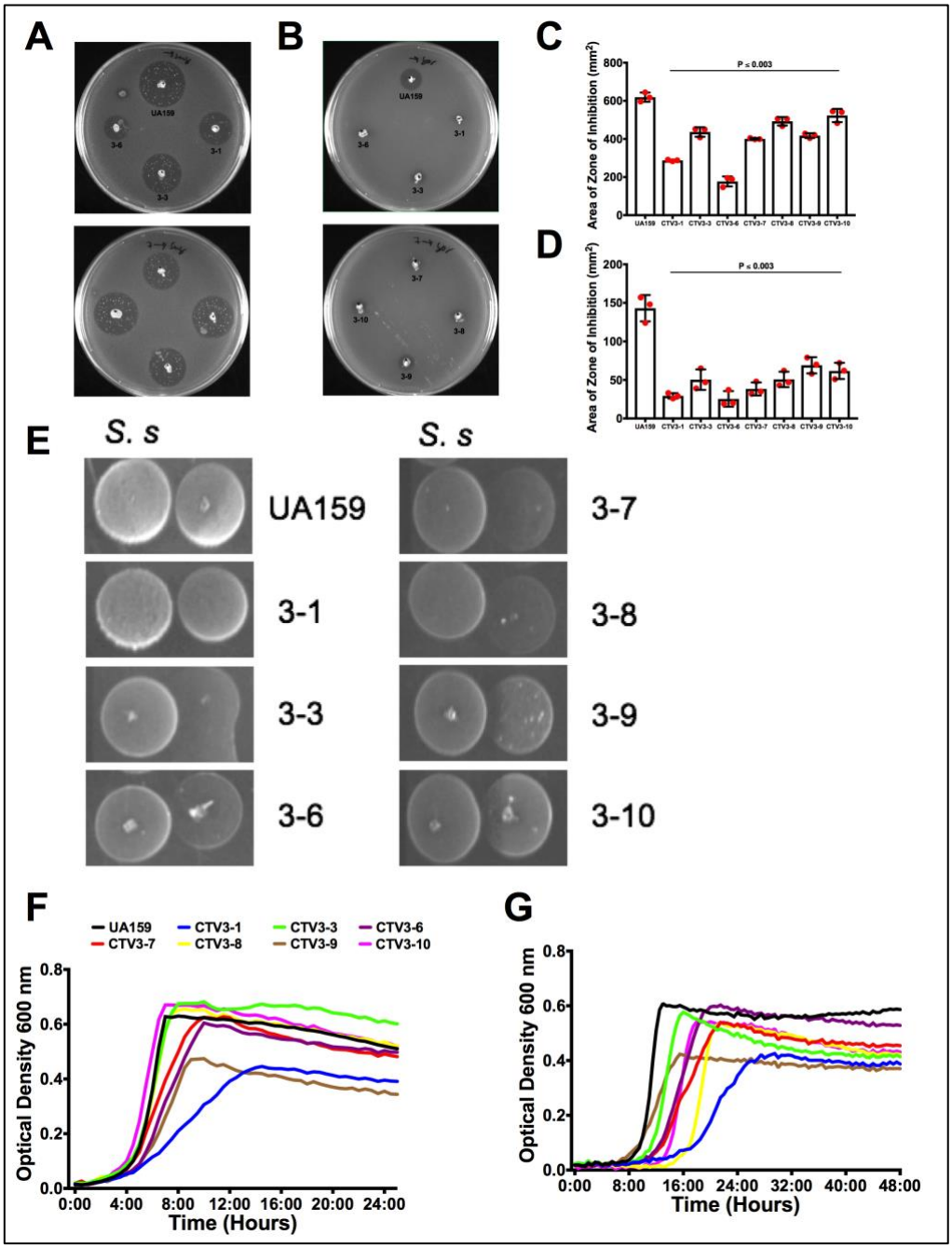

Figure 4. Competition of CTV3s against oral streptococci. Agar plate images of bacteriocin overlay assays displaying zones of inhibition against indicator strain (A) *S. sanguinis* SK150 and (B) *S. gordonii* DL1. Quantification of bacteriocin overlay assays using measured zones of inhibition against indicator strain (C) *S. sanguinis* SK150 and (D) *S. gordonii* DL1. Quantification was conducted using the ImageJ measuring tool and represents the average of three replicates from two independent experiments. All CTV3 zones of inhibition were statistically significant from parental UA159 (P value ≤ 0.003). (E) Agar plate competition assay between *S. sanguinis* SK150 (labeled S. s, left colony) and either the parental strain UA159 or the CTV3s (right colony). Colonies were spotted at the same time and grown for 48 h prior to imaging. Growth of the parental UA159 strain (black line) and each of the CTV3s (colored lines) in either (F) 0.001% H_2O_2 or (G) 0.003% H_2O_2.

Whole Genome Sequencing Reveals Mutations in CTVs.

To determine what mutations are carried in each of the characterized CTV3s, whole genome sequencing was performed on extracted chromosomal DNA as described in the material and methods section. Our analysis for single nucleotide polymorphisms (SNPs) revealed four genes of interest that carried mutations in at least three or more of the sequenced CTV3s. The presence of the SNPs were confirmed by PCR and sequencing in SMU.804, SMU.1542c, SMU.1576c and SMU.1588c.

The only gene within the genome to carry SNPs in all seven of the sequenced CTV3s was SMU.1542c **(Table 3)**. SMU.1542c is homologous to *dgkB* (*yerQ*) of *Bacillus subtilis*, a

soluble diacylglycerol kinase (DGK) that phosphorylates diacylglycerol (DAG) generated by the transfer of the *sn*-1-glycerol-P headgroup from phosphatidylglycerol to lipoteichoic acid (LTA) (27, 28). Intriguingly, DgkB from *B. subtilis* is essential for growth, yet four different non-synonymous SNPs were identified between our seven sequenced CTV3s that occurred over the length of the gene and were not confined to one particular region. It is not known whether the lethality of the loss of *dgkB* in *B. subtilis* is due to accumulation of toxic DAG in the membranes or from the absence of LTA (28). We suspected that the resulting non-synonymous SNPs in the apparent *S. mutans dgkB* homologue in CTV3s may result in changes to the efficiency of the enzyme, rather than complete loss of function. To test this hypothesis, we performed a western blot on the extracted LTA from the parental strain and the CTV3s **(Figure 5A)**. Differential accumulation of LTA in the CHX tolerant strains were noted. CTV3-1 and CTV3-10 appeared to accumulate more LTA and CTV3s 6, 7, 8 and 9 accumulated less LTA than the wild-type strain. Thus, it does appear that our CTV3s show different patterns in the amount of LTA produced that may be related to the SNPs. Further analysis will be required to determine if the LTA and lipid profiles are altered in the CTV3s, as has been reported for *E. faecium* (19) with elevated CHX tolerance.

We analyzed the SNPs occurring within *dgkB* of our CTV3s to determine how they might affect DgkB function within *S. mutans* by comparing to characterized Dgk enzymes, including the lipid kinase YegS from *Escherichia coli*, DgkB of *Staphylococcus aureus* of which the structure has been solved (27), as well as the ten known isoforms of human DGKs **(Supplemental Figure 2)**. We noted that the amino acid (aa) substitution G131S occurring within CTV3s 6, 7 and 9 arose within beta sheet 6 and was a naturally occurring substitution found within human cerimide kinase CERK, a member of the DGK superfamily (Pfam00781). The mutation causing G164D, found in CTV3-1, was a substitution occurring within DGKζ, a human type-2 DGK. Substitution D249E found in CTV3-3 occurred at the end of alpha helix 7 and is present in YegS of *E. coli*. Finally, aa substitution A304D of CTV3-8 and CTV3-10 occurred within a conserved residue of the DGKs (27) after beta sheet 17, with no known symmetry between the DGKs examined. None of the aa substitutions were within regions of the protein that impacted nucleotide (ATP/ADP) -binding regions nor along the DgkB dimerization interface. Therefore, we are unable to postulate how the identified SNPs of the CTV3s within SMU.1542c may alter the function of DgkB. However, since a majority of the SNPs lead to amino acid substitutions found in other DgkB homologs, combined with the fact that these SNPs do not lead to abberant growth defects in their respective variant, as demonstrated using multiple growth tests, we assume that the DgkB enzyme in the CTV3s is still functional.

SMU.1588c is annotated to be a glycolipid synthesis enzyme, specifically a 1,2-diacylglycerol 3-glucosyltransferase that synthesizes glucose(α1-3)-DAG from uridine diphosphate glucose (UDP-glucose) and termed *lafA* in *Listeria monocytogenes* (29). It is encoded within an operon with SMU.1589c that shares homology to *lafB* of *L. monocytogenes*, responsible for the addition of a galactose moiety to form galctosyl-(α1-2)-glucosyl-(α1-3)-DAG using UDP-galactose as a substrate. In *Streptococcus agalactiae*, the LTA anchor is α1-2 linked Glu_2-DAG and is produced by a two-enzyme system similar to L. *monocytogenes* (30–32). We encountered two different non-synonymous SNPs within the *lafA* homolog SMU.1588c: 1) aa substitution P433A in CTV3-6 and CTV3-8, and 2) W391STOP, which leads to truncation of the protein at aa 391. Interestingly, the protein sequence of the well characterized *Acholeplasma laidlawii* 1,2-diacylglycerol 3-glucosyltransferase also ends at position 391 when the protein sequences are aligned **(Figure 5B)**. It is unknown what function the additional C-terminal amino acids of the *S. mutans* 1,2-diacylglycerol 3-glucosyltransferase might serve, but the additional domain(s) is present in *Streptococcus*, *Staphylococcus*, *Enterococcus* and *Listeria,* but not in *Bacillus*.

Two other genes, SMU.804 and SMU.1576c, were found to have SNPs in three of the CTV3s. CTV3s 7, 8 and 10 harbored SNPs in SMU.804, while CTV3s 7, 8 and 9 harbored SNPs in SMU.1576c. Both genes are listed as hypothetical proteins with no known function. To determine if these two genes may be involved in a CHX-tolerant phenotype that is observed in our variants, we individually replaced each gene with a non-polar kanamycin antibiotic marker to create strains Δ804 and Δ1576c. The mutant strains did not display any changes in growth compared to the parental strain when grown in 0.50 μg mL $^{-1}$ or 0.75 μg mL $^{-1}$ CHX, nor did the loss of either gene impact the strain's MIC to daptomycin or change antagonistic interactions with commensal streptococci as assessed with the bacteriocin overlay and plate-based competition assays **(Supplemental Figure 3)**. Together, these data suggest that while SNPs accumulated in both of these genes in three different variants, they were either not solely responsible for the phenotypes of the variants and/or the mutations did not cause complete loss of function.

Other intriguing SNPs **(Supplemental Table 1)**, such as those found in the *rcrP* gene of CTV3-1 (33) or the *rcrRPQ* peptides of CTV3-7 (34) were documented. The *rcrRPQ* operon and two peptides encoded in *rcrQ* play major roles in stress tolerance and genetic competence, but SNPs in *rcrRPQ* occurred in only one of the variants sequenced. We cannot rule out, however, that these single SNPs or a combinatorial effect of the multiple SNPs in individual variants are responsible for the observed phenotypes. However, we have been unable to assign direct causation of the displayed phenotypes by any particular SNP. A future study designed to assess global transcriptomic changes in the variants compared to the parental strain may help to resolve the basis for enhanced resistance to growth inhibition by CHX and may provide valuable insights into mechanisms of action of the compound and ways to enhance its efficacy in oral biofilm control.

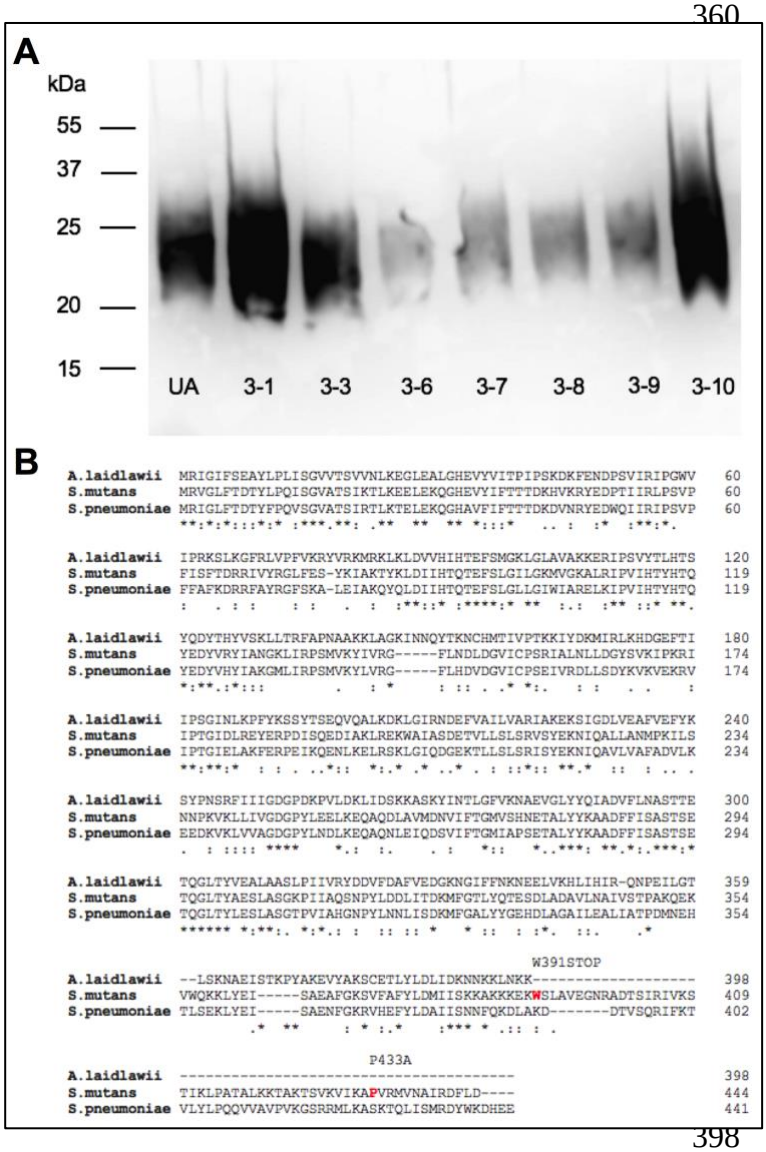

Figure 5. CTV3s SNPs associate with changes in LTA. (A) Western blot of parental UA159 and the CTV3s using a 1:5000 dilution of Gram-positive bacterial LTA monoclonal antibody. Cells were grown in BHI medium to late exponential log phase ($OD_{600\ nm}$ ~ 0.8) prior to harvest. LTA was extracted by adding 500 μL of 2x sample buffer to 0.1 g of cell pellet and boiling for 1 hr. 10 μL was then added to a 4-20% TGX pre-cast protein gel. Molecular mass standards (in kDa) are shown to the left. (B) Amino acid (aa) alignment (Clustal Omega) between the *lafA* gene (SMU.1588c) of *A. laidlawii, S. mutans*, and *S. pneumoniae* (*D39*, spd_0961). Red bolded aa within the *S. mutans* sequence signify those residues that were found to be mutated within the CTV3s by whole genome sequence analysis, with the corresponding amino acid substitution found above. STOP = stop codon. Sequences were aligned using the web tool Clustal Omega (https://www.ebi.ac.uk/Tools/msa/clustalo/).

Table 3. SMU.1542c Mutations in CTV3s

CTV Strain Containing Mutation	Genome SNP*	Genome Position[%]	1542c Location[$]	1542c SNP^	1542c aa Location[&]	1542c aa Change[+]
6, 7, 9	c > t	1471014	391	g > a	131	G > S
8, 10	g > t	1470494	911	c > a	304	A > D
1	c > t	1470914	491	g > a	164	G > D
3	c > t	1470659	746	g > a	249	G > E

[*]Refers to the base change on the forward chromosome strand; 1542c is encoded in the reverse orientation
[%]Location of the base pair that encodes the SNP in reference to the entire genome
[$]Location of the base pair that encodes the SNP in reference to the 1542c gene alone
[^]Refers to the base change on the reverse chromosome strand in which 1542c is encoded
[&]Location of the amino acid that encodes the SNP in reference to the 1542c gene alone
[+]Refers to the amino acid change within the 1542c coding sequence due to the SNP

Table 4. SMU.1588c Mutations in CTV3s

CTV Strain Containing Mutation	Genome SNP[*]	Genome Location[%]	1588c Location[$]	1588c SNP[^]	1588c aa Location&	1588c aa Change[+]
6, 8	g > c	1518523	1295	c > g	433	P > A
10	c > t	1518644	1174	g > a	391	W > STOP

[*]Refers to the base change on the forward chromosome strand; 1542c is encoded in the reverse orientation
[%]Location of the base pair that encodes the SNP in reference to the entire genome
[$]Location of the base pair that encodes the SNP in reference to the 1542c gene alone
[^]Refers to the base change on the reverse chromosome strand in which 1542c is encoded
[&]Location of the amino acid that encodes the SNP in reference to the 1542c gene alone
[+]Refers to the amino acid change within the 1542c coding sequence due to the SNP

SUMMARY

The use of antimicrobials in either mouthwashes or dentifrices in conjunction with standard mechanical removal of oral biofilms through brushing has been common practice in the dental setting for several decades. Still today, use of antimicrobials such as CHX in varnishes or even incorporation of CHX in nanoparticles is being proposed for treatments to reduce the appearance of white spot lesions in patients with fixed orthodontic appliances. Even though CHX has been commonplace in the dental setting for decades, we still know very little about its mode of action against cariogenic bacteria, such as *S. mutans,* and whether or not a tolerant and/or resistant phenotype against CHX can arise and the consequences that brings to the homeostasis of the oral microbiome. The work reported here finally begins to explore these issues and finds that after only a few rounds of passaging on CHX-containing agar can spontaneously-arising variants develop with increased tolerance to CHX. However, further investigation and characterization of these variants determines that while these variants do in fact have the potential to tolerate and persist at low pH values, tolerance to CHX comes at a fitness cost to the bacteria in terms of being able to compete against other commensal streptococci within oral biofilms, as well as increased susceptibility to other common oral antimicrobials such as triclosan and sodium fluoride.

While broad-spectrum antimicrobials that reduce the overall bacterial load will most likely always be commonplace in the healthcare setting, the increase in antimicrobial resistance to common antibiotics and the realization that removal of the natural flora can have unintended consequences, including allowing pathogens into the unoccupied niche(s) necessitate continuing the search for novel preventive and therapeutic interventions. The unintended finding that chlorhexidine tolerance through accumulated SNPs can lead to increased susceptibility to triclosan and sodium fluoride opens the door to future research in determining the mechanisms of action for designation of a drug target that complements existing treatments. Together, a

focus on these mechanistically-driven studies in microbial physiology and genetics will strengthen our knowledge base, provide novel insights into how we can more effectively target cariogenic bacteria, and translate to better health outcomes in the clinic to increase our quality of life.

MATERIALS and METHODS

Bacterial Strains and Growth Conditions.

S. mutans wild-type strain UA159 and its derivatives **(Supplemental Table 2)** were grown in either brain heart infusion (BHI – Difco) or FMC (35) medium. The medium was supplemented with 1 mg ml^{-1} of kanamycin when needed. Unless otherwise noted, cultures were grown overnight in BHI medium with the appropriate antibiotics at 37°C in a 5% CO_2 aerobic atmosphere. The next day, cultures were harvested by centrifugation, washed twice in 1 mL of phosphate-buffered saline (PBS), and resuspended in PBS to remove all traces of BHI. Cells were then diluted in the desired medium before beginning each experiment. For growth rate comparisons, overnight cultures were diluted 1:50 and grown to mid-exponential phase (OD_{600} = 0.5–0.6). Then, cultures were re-diluted 1:100 into 300 µl of BHI and added to multiwell plates along with any condition to be tested (0.75 µg ml^{-1} CHX, 8 and 16 µg ml^{-1} Triclosan, 100 and 300 µg ml^{-1} NaF, and 0.001% and 0.003% H_2O_2). Cultures were overlaid with 50 µl of sterile mineral oil to reduce the growth inhibitory effects of air on growth of *S. mutans*. The optical density at 600 nm (OD_{600}) was monitored at 30 min intervals for 24 h using a Bioscreen C lab system (Helsinki, Finland) at 37◦C with shaking for 10 s before each reading. Three biological replicates measured in technical triplicates was measured for each experiment and the averaged growth rates of the replicates was used to calculate doubling times and final yields.

Passaging of S. mutans on BHI Agar Plates Containing CHX.

S. mutans wild-type strain UA159 was first grown overnight in BHI medium. The next morning, the overnight cultures were diluted 1:50 and grown to mid-exponential growth phase (OD_{600} = 0.5–0.6) before being back-diluted to $1X10^6$ CFU. The $1X10^6$ CFU was then plated on BHI agar plates containing either 0.1, 0.25 or 0.50 µg ml^{-1} CHX (> 99.5%, Sigma-Aldrich). The colonies returned on these BHI agar plates was considered the first generation (CTV1s). 10 selected colonies that appeared on the 0.50 µg ml^{-1} CHX plate were then chosen for overnight inoculation to repeat the process. For the second generation, $1X10^6$ CFU of each outgrowth was then plated on 10 separate BHI agar plates containing either 0.75, 1.0 or 1.25 µg ml^{-1} CHX. One single colony from each of the 10 agar plates containing 1.25 µg ml^{-1} CHX was then chosen for overnight inoculation to repeat the process for a third and final time. $1X10^6$ CFU of each outgrowth grown to mid-exponential growth phase was then plated on 10 separate BHI agar plates containing either 1.5, 1.625 or 1.75 µg ml^{-1} CHX. One single colony from each of the 10 agar plates containing 1.75 µg ml^{-1} CHX was then selected to be further characterized.

Microtiter Plate Growth Assays.

CHX concentrations to be tested were first added to BHI medium with addition of DMSO only serving as a negative control. 198 µl of each concentration was then pipetted across a row of a 96-well microtiter plate. Next, 2 µl of either *S. mutans* wild-type strain UA159 or its derivative to be tested grown to mid-exponential growth phase (OD_{600} = 0.5–0.6) in BHI medium was used to inoculate the wells of the plate. The OD_{600} of the cultures was measured after 24 h incubation at 37°C in a 5% CO_2 aerobic atmosphere with a Synergy 2 multimode microplate reader (BioTek). The experiment was performed at least three times.

Competitive Fitness Index Assays.

To determine fitness of the CTV3 s, cultures were grown overnight alongside *S. mutans* wild-type strain UA159 and UA159 harboring the chromosomally-integrated vector pMC304B

that carries an antibiotic resistant kanamycin cassette which can be used for selection purposes. The next day, all strains were grown to mid-exponential growth phase (OD_{600} = 0.5–0.6) after a 1:50 dilution from the overnights. A 1:1000 dilution from the mid-exponential growth phase cultures was then used to inoculate 1 mL of BHI in which either the CTV3s or wild-type UA159 were competed against UA159 harboring pMC304B. At this time, a small aliquot was serially diluted and plated on either BHI (total cell count) or BHI containing 1 mg ml^{-1} kanamycin (UA159 harboring pMC304B count) to determine initial cell count at the beginning of the experiment. After 24 h of growth at 37°C in a 5% CO_2 aerobic atmosphere, cultures were again serially diluted and plated to determine final cell count. All colony forming units (CFUs) were counted after 48 h of agar plate incubation at 37°C in a 5% CO_2 aerobic atmosphere. To determine the cell count of either the CTV3s or wild-type UA159, the UA159 harboring pMC304B count was subtracted from the total cell count. The competitive fitness index from the perspective of either the CTV3s or wild-type UA159 was calculated with the following equation: Log10((CTV3 cell count $_{final}$ / UA159 cell count $_{final}$) / (CTV3 cell count $_{initial}$ / UA159 cell count $_{initial}$). This experiment was repeated twice with three biological replicates for each experiment.

Measurements of Biofilm Biomass.

Selected strains were grown from overnight cultures to mid-exponential phase after a 1:20 dilution in CDM broth at 37ºC in a 5% CO_2 atmosphere. The mid-exponential phase cells were then diluted 1:100 into CDM medium with either 20 mM glucose or CDM medium containing 15 mM glucose and 2.5 mM sucrose as a carbohydrate source. 200 µL of this dilution was loaded into 96 well polystyrene microtiter plates and incubated in a 5% CO_2 atmosphere at 37ºC for 48 h. After, the medium was decanted, and the plates were washed twice with 200 µL of sterile water to remove planktonic and loosely bound cells. The adherent bacteria were stained with 60 µL of 0.1% crystal violet for 15 min. After rinsing twice with 200 µL of water, the bound dye was extracted from the stained biofilm using 200 µL of ethanol:acetone (8:2) solution, twice. The extracted dye was diluted into 1.6 mL of ethanol:acetone solution. Biofilm formation was quantified by measuring the absorbance of the solution at OD 575 nm. For determination of percent change, the value of wild-type UA159 was set to 100% for either the glucose-only or glucose/sucrose grown biofilms. This experiment was repeated twice with 3 independent biological replicates with 4 technical replicates each.

ETEST Antibiotic Susceptibility Testing.

Selected strains were grown from overnight cultures to mid-exponential phase after a 1:20 dilution in BHI broth at 37ºC in a 5% CO_2 atmosphere. 10 µL from the mid-exponential culture was then added to 10 mL soft BHI agar (0.75% agarose) and overlaid on to BHI agar plates. Once solidified, ETEST strips (bioMérieux, Inc., Durham, N.C.) containing either Amoxicillin, Azithromycin, Bacitracin, Clindamycin, Daptomycin or Vancomycin when then laid over the agar with sterile forceps. After 48 h of growth at 37°C in a 5% CO_2 aerobic atmosphere, the agar plates were examined, imaged and lowest MIC recorded where no growth was visible. Two independent observers (J.K. and M.G.) interpreted the agar dilution and ETEST MICs. While a specific blinding protocol was not used, neither observer had knowledge of the other's measurements prior to making their own MIC determinations. Discrepancies were resolved by consensus. Each strain was plated three times from three independent biological replicates.

Bacteriocin Overlay Assays.

Selected strains were grown from overnight cultures to mid-exponential phase after a 1:20 dilution in BHI broth at 37ºC in a 5% CO_2 atmosphere. Using a toothpick, the strains were stabbed into BHI agar and incubated for 24 h in a 5% CO2 atmosphere at 37°C. The following day, 10 mL soft BHI agar (0.75% agarose) was inoculated with either 10 µL *Streptococcus*

546 *sanguinis* SK150 or *Streptococcus gordonii* DL1 overnight culture. The soft agar with bacterial
547 indicator strain was overlaid onto the BHI agar plates with stabbed *S. mutans* colonies. After 24
548 h, plates were imaged and zones of clearance were calculated using ImageJ image analysis
549 software. This experiment was repeated twice with three independent biological replicates in
550 each experiment. Statistical analysis was performed using the Student's T-Test.
551
552 *Agar Spot Competition Assays.*
553 Selected strains were grown from overnight cultures to mid-exponential phase after a
554 1:20 dilution in BHI broth at 37ºC in a 5% CO_2 atmosphere. Each strain (7 µL) was then
555 inoculated adjacent to one another on agar plates as follows: *S. sanguinis* SK150 first and to the
556 left, followed by S. mutans UA159 or CTV3 strains after the SK150 spot has dried. The plates
557 were incubated for 48 h at 37°C, in 5% CO_2 prior to imaging. This experiment was repeated
558 twice with three independent biological replicates in each experiment.
559
560 *Construction of Bacterial Strains.*
561 Mutant strains of *S. mutans* **(Supplemental Table 3)** were created using a PCR ligation
562 mutagenesis approach as previously described (Lau *et al.*, 2002). Briefly, 700 bp fragments
563 both upstream and downstream of the gene of interest were amplified with designed primers
564 and containing a BamHI restriction site in the region closest to the gene. After restriction digest,
565 a non-polar kanamycin resistant cassette was ligated within the arms. This ligated fragment was
566 then transformed into *S. mutans* UA159 with selection on BHI agar containing 1 mg mL^{-1}
567 kanamycin. Successful replacement was confirmed both by size selection colony PCR and
568 Sanger sequencing (Eurofins Genomics, Louisville, KY, USA). Restriction and DNA-modifying
569 enzymes were obtained from New England Biolabs. PCRs were carried out with 100 ng of
570 chromosomal DNA by using *Taq* DNA polymerase, and PCR products were purified with the
571 QIAquick kit (QIAGEN).
572
573 *Whole Genome Sequencing and SNP Calling.*
574 For whole genome shotgun sequencing, genomic DNA were isolated from both the
575 parental UA159 and each of the seven CTV3s using Wizard® Genomic DNA Purification Kit
576 (Promega, Madison, WI, USA) with some modifications. The total cell lysate from 10 mL of
577 overnight cultures grown in BHI was then harvested and the supernatant containing the DNA
578 sample was transferred to a fresh tube containing room temperature isopropanol. The
579 supernatant was rotated at room temperature about an hour or until the thread-like strands of
580 DNA formed a visible mass. DNA was purified in nuclease-free water after two washes in 70%
581 ethanol. Total DNA concentration was measured using a NanoDrop™ One Microvolume UV-Vis
582 Spectrophotometer (ThermoFisher Scientific, Waltham, MA, USA) and DNA integrity was
583 determined by 260/280 ratio. 2-5 ng of DNA from each variant was prepared for next-generation
584 whole genome shotgun sequencing using the Illumina Nextera-XT library preparation and
585 indexing kit. Libraries were normalized by hand rather than with the Nextera-XT kit beads, and
586 were pooled at a final concentration of 2 nM and sequenced on an Illumina MiSeq using the
587 Illumina MiSeq v2 kit with paired-end sequencing and 250-bp reads. Reads were de-multiplexed
588 by the Illumina 468 software. The pipeline a5 (38) was used to remove adapters from, quality-
589 trim, and assemble the raw fastq files into contigs, using default settings. The quality of
590 assembled genomes was checked using QUAST (39). The assembled contigs from each
591 respective variant were pairwise aligned against the deposited GenBank *S. mutans* UA159 file
592 (http://www.ncbi.nlm.nih.gov/nuccore/NC_004350.2) using the Mauve multiple genome
593 alignment tool (version 2.4.0) (40) and SNPs unique to that variant from the parental were called
594 through visual inspection. SNPs in genes SMU.804, SMU.1542c, SMU.1576c and SMU.1588c
595 were confirmed via Sanger sequencing (Eurofins Genomics, Louisville, KY, USA)
596 (Supplemental Table 3). The raw reads from all genomes we sequenced for this study are

available to download from the NCBI SRA under accession numbers SAMN10743465 – SAMN10743475 **(Supplemental Table 4)**.

Western blotting.

Bacterial strains were grown in BHI at 37°C until they reached an $OD_{600\ nm}$ ~ 0.8. Cells were harvested by centrifugation at 3500 g for 10 min, spent media was discarded, and cell pellets were stored overnight at -20°C. The following day, pellets were re-suspended in 500 µL 2X SDS sample buffer (100 mM Tris, pH 6.8, 4% SDS, 20% glycerol, 0.004% bromophenol blue, 10% 2-mercaptoethanol) corresponding to 0.1 g of cell pellet weight. The resuspension was then boiled for 1 h. Following, the remaining debris was sedimented by centrifugation and ten µL of each sample was loaded onto a 4-20% precast TGX protein gel (BioRad). Protein samples were separated by SDS-polyacrylamide gel electrophoresis (SDS-PAGE) and then transferred to a polyvinylidene difluoride (PVDF) membrane using a Trans-Blot® Turbo™ Transfer System (BioRad). LTA was detected using a Gram-positive Bacteria LTA monoclonal antibody (1:5000 primary dilution; Thermo Fisher Scientific) and a goat-anti-mouse immunoglobulin G (IgG) antibody (1:5000 dilution; SeraCare Life Sciences, USA). Western blot signals were detected using the SuperSignal™ West Pico Chemiluminescent Substrate kit (Thermo Fisher Scientific) and visualized with a FluorChem 8900 imaging system (Alpha Innotech, USA).

ACKNOWLEDGEMENTS

We thank Dr. Robert Shields for assistance with the SNP analysis and for thoughtful discussions related to the manuscript. Research reported in this publication was supported by the National Institute of Dental and Craniofacial Research of the National Institutes of Health under Award Numbers R01 DE023339, R01 DE13239, and T90 DE21990.

REFERENCES

1. **Pitts NB**, **Zero DT**, **Marsh PD**, **Ekstrand K**, **Weintraub JA**, **Ramos-Gomez F**, **Tagami J**, **Twetman S**, **Tsakos G**, **Ismail A**. 2017. Dental caries. Nat Rev Dis Prim **3**:17030.
2. **Wang Y**, **Li J**, **Sun W**, **Li H**, **Cannon RD**, **Mei L**. 2017. Effect of non-fluoride agents on the prevention of dental caries in primary dentition: A systematic review. PLoS One **12**:e0182221.
3. **Duangthip D**, **Jiang M**, **Chu CH**, **Lo EC**. 2015. Non-surgical treatment of dentin caries in preschool children – systematic review. BMC Oral Health **15**:44.
4. **Autio-Gold J**. 2008. The Role of Chlorhexidine in Caries Prevention. Oper Dent **33**:710–716.
5. **Lee D-W**, **Jung J-E**, **Yang Y-M**, **Kim J-G**, **Yi H-K**, **Jeon J-G**. 2016. The antibacterial activity of chlorhexidine digluconate against *Streptococcus mutans* biofilms follows sigmoidal patterns. Eur J Oral Sci **124**:440–446.
6. **Liu J**, **Ling J-Q**, **Zhang K**, **Huo L-J**, **Ning Y**. 2012. Effect of sodium fluoride, ampicillin, and chlorhexidine on *Streptococcus mutans* biofilm detachment. Antimicrob Agents Chemother **56**:4532–5.
7. **Jeon J-G**, **Rosalen PL**, **Falsetta ML**, **Koo H**. 2011. Natural products in caries research: current (limited) knowledge, challenges and future perspective. Caries Res **45**:243–63.
8. **Gilbert P**, **Moore LE**. 2005. Cationic antiseptics: diversity of action under a common epithet. J Appl Microbiol **99**:703–715.
9. **Cheung H-Y**, **Wong MM-K**, **Cheung S-H**, **Liang LY**, **Lam Y-W**, **Chiu S-K**. 2012. Differential Actions of Chlorhexidine on the Cell Wall of *Bacillus subtilis* and *Escherichia coli*. PLoS One **7**:e36659.

10. **Järvinen H**, **Tenovuo J**, **Huovinen P**. 1993. *In vitr*o susceptibility of *Streptococcus mutans* to chlorhexidine and six other antimicrobial agents. Antimicrob Agents Chemother **37**:1158–9.
11. **Bhardwaj P**, **Ziegler E**, **Palmer KL**. 2016. Chlorhexidine Induces VanA-Type Vancomycin Resistance Genes in Enterococci. Antimicrob Agents Chemother **60**:2209–21.
12. **Guzmán Prieto AM**, **Wijngaarden J**, **Braat JC**, **Rogers MRC**, **Majoor E**, **Brouwer EC**, **Zhang X**, **Bayjanov JR**, **Bonten MJM**, **Willems RJL**, **van Schaik W**. 2017. The Two-Component System ChtRS Contributes to Chlorhexidine Tolerance in *Enterococcus faecium*. Antimicrob Agents Chemother **61**:AAC.02122-16.
13. **Waites KB**, **Figarola TA**, **Schmid T**, **Crabb DM**, **Duffy LB**, **Simecka JW**. 1991. Comparison of agar versus broth dilution techniques for determining antibiotic susceptibilities of *Ureaplasma urealyticum*. Diagn Microbiol Infect Dis **14**:265–271.
14. **Belli WA**, **Marquis RE**. 1991. Adaptation of *Streptococcus mutans* and *Enterococcus hirae* to acid stress in continuous culture. Appl Environ Microbiol **57**:1134–8.
15. **Hamilton IR**, **St Martin EJ**. 1982. Evidence for the involvement of proton motive force in the transport of glucose by a mutant of *Streptococcus mutans* strain DR0001 defective in glucose-phosphoenolpyruvate phosphotransferase activity. Infect Immun **36**:567–75.
16. **Marsh PD**. 2003. Are dental diseases examples of ecological catastrophes? Microbiology **149**:279–294.
17. **Fozo EM**, **Quivey RG**. 2004. Shifts in the membrane fatty acid profile of *Streptococcus mutans* enhance survival in acidic environments. Appl Environ Microbiol **70**:929–36.
18. **Liu Y**, **Zeng L**, **Burne RA**. 2009. AguR is required for induction of the *Streptococcus mutans* agmatine deiminase system by low pH and agmatine. Appl Environ Microbiol **75**:2629–37.
19. **Bhardwaj P**, **Hans A**, **Ruikar K**, **Guan Z**, **Palmer KL**. 2018. Reduced Chlorhexidine and Daptomycin Susceptibility in Vancomycin-Resistant *Enterococcus faecium* after Serial Chlorhexidine Exposure. Antimicrob Agents Chemother **62**:e01235-17.
20. **Renzoni A**, **Von Dach E**, **Landelle C**, **Diene SM**, **Manzano C**, **Gonzales R**, **Abdelhady W**, **Randall CP**, **Bonetti EJ**, **Baud D**, **O'Neill AJ**, **Bayer A**, **Cherkaoui A**, **Schrenzel J**, **Harbarth S**, **François P**. 2017. Impact of Exposure of Methicillin-Resistant *Staphylococcus aureus* to Polyhexanide *In Vitro* and *In Vivo*. Antimicrob Agents Chemother **61**:e00272-17.
21. **Wilson DN**. 2014. Ribosome-targeting antibiotics and mechanisms of bacterial resistance. Nat Rev Microbiol **12**:35–48.
22. **Blinkhorn A**, **Bartold PM**, **Cullinan MP**, **Madden TE**, **Marshall RI**, **Raphael SL**, **Seymour GJ**. 2009. Is there a role for triclosan/copolymer toothpaste in the management of periodontal disease? Br Dent J **207**:117–125.
23. **Bender GR**, **Thibodeau EA**, **Marquis RE**. 1985. Reduction of acidurance of streptococcal growth and glycolysis by fluoride and gramicidin. J Dent Res **64**:90–5.
24. **Liao Y**, **Brandt BW**, **Li J**, **Crielaard W**, **Van Loveren C**, **Deng DM**. 2017. Fluoride resistance in *Streptococcus mutans* : a mini review. J Oral Microbiol **9**:1344509.
25. **Bowen WH**, **Burne RA**, **Wu H**, **Koo H**. 2017. Oral Biofilms: Pathogens, Matrix, and Polymicrobial Interactions in Microenvironments. Trends Microbiol.
26. **Kreth J**, **Zhang Y**, **Herzberg MC**. 2008. Streptococcal antagonism in oral biofilms: *Streptococcus sanguinis* and *Streptococcus gordonii* interference with *Streptococcus mutans*. J Bacteriol **190**:4632–40.
27. **Miller DJ**, **Jerga A**, **Rock CO**, **White SW**. 2008. Analysis of the *Staphylococcus aureus* DgkB Structure Reveals a Common Catalytic Mechanism for the Soluble Diacylglycerol Kinases. Structure **16**:1036–1046.
28. **Jerga A**, **Lu Y-J**, **Schujman GE**, **de Mendoza D**, **Rock CO**. 2007. Identification of a

soluble diacylglycerol kinase required for lipoteichoic acid production in *Bacillus subtilis*. J Biol Chem **282**:21738–45.

29. **Webb AJ**, **Karatsa-Dodgson M**, **Gründling A**. 2009. Two-enzyme systems for glycolipid and polyglycerolphosphate lipoteichoic acid synthesis in *Listeria monocytogenes*. Mol Microbiol **74**:299–314.
30. **Reichmann NT**, **Gründling A**. 2011. Location, synthesis and function of glycolipids and polyglycerolphosphate lipoteichoic acid in Gram-positive bacteria of the phylum Firmicutes. FEMS Microbiol Lett **319**:97–105.
31. **Theilacker C**, **Sanchez-Carballo P**, **Toma I**, **Fabretti F**, **Sava I**, **Kropec A**, **Holst O**, **Huebner J**. 2009. Glycolipids are involved in biofilm accumulation and prolonged bacteraemia in *Enterococcus faecalis*. Mol Microbiol **71**:1055–1069.
32. **Doran KS**, **Engelson EJ**, **Khosravi A**, **Maisey HC**, **Fedtke I**, **Equils O**, **Michelsen KS**, **Arditi M**, **Peschel A**, **Nizet V**. 2005. Blood-brain barrier invasion by group B *Streptococcus* depends upon proper cell-surface anchoring of lipoteichoic acid. J Clin Invest **115**:2499–507.
33. **Seaton K**, **Ahn S-J**, **Sagstetter AM**, **Burne RA**. 2011. A transcriptional regulator and ABC transporters link stress tolerance, (p)ppGpp, and genetic competence in *Streptococcus mutans*. J Bacteriol **193**:862–74.
34. **Ahn S-J**, **Kaspar J**, **Kim JN**, **Seaton K**, **Burne R a**. 2014. Discovery of novel peptides regulating competence development in *Streptococcus mutans*. J Bacteriol **196**:3735–3745.
35. **Chang JC**, **LaSarre B**, **Jimenez JC**, **Aggarwal C**, **Federle MJ**. 2011. Two Group A Streptococcal Peptide Pheromones Act through Opposing Rgg Regulators to Control Biofilm Development. PLoS Pathog **7**:e1002190.
36. **Lau PC.**, **Sung CK**, **Lee JH**, **Morrison DA**, **Cvitkovitch DG**. 2002. PCR ligation mutagenesis in transformable streptococci: application and efficiency. J Microbiol Methods **49**:193–205.
37. **Kaspar J**, **Ahn S-J**, **Palmer SR**, **Choi SC**, **Stanhope MJ**, **Burne RA**. 2015. A Unique ORF within the *comX* gene of *Streptococcus mutans* Regulates Genetic Competence and Oxidative Stress Tolerance. Mol Microbiol **96**:463–482.
38. **Tritt A**, **Eisen JA**, **Facciotti MT**, **Darling AE**. 2012. An Integrated Pipeline for *de Novo* Assembly of Microbial Genomes. PLoS One **7**:e42304.
39. **Gurevich A**, **Saveliev V**, **Vyahhi N**, **Tesler G**. 2013. QUAST: quality assessment tool for genome assemblies. Bioinformatics **29**:1072–1075.
40. **Darling AE**, **Tritt A**, **Eisen JA**, **Facciotti MT**. 2011. Mauve Assembly Metrics. Bioinformatics **27**:2756–2757.

Table S1. SNPs of the CTV3s.

CTV3-1						
Number	SNP pattern	Gene	Name	Function	Location	
1	ct	SMU.922	*rcrP*	ABC transporter	NC_004350	875439
2	at	SMU.974	*potB*	putative spermidine/putrescine ABC transporter	NC_004350	920843
3	ct	SMU.1542c		lipid kinase	NC_004350	1470914
CTV3-3						
Number	SNP pattern	Gene	Name	Function	Location	
1	ca	SMU.577	*lytS*	histidine kinase	NC_004350	540225
2	ga	SMU.895		DNA damage inducible protein	NC_004350	849956
3	ct	SMU.1344c		malonyl-CoA acyl-carrier protein transacylase	NC_004350	1284607
4	ct	SMU.1542c		lipid kinase	NC_004350	1470659
5	ga	SMU.1989c	*rpoC*	DNA-directed RNA polymerase	NC_004350	1857079
CTV3-6						
Number	SNP pattern	Gene	Name	Function	Location	
1	ag	IGR SMU.685 - SMU.687c		hypothetical protein	NC_004350	652281
2	gc	SMU.1004	*gtfB*	glucosyltransferase	NC_004350	953114
3	tg	SMU.1004	*gtfB*	glucosyltransferase	NC_004350	953123
4	gt	SMU.1004	*gtfB*	glucosyltransferase	NC_004350	953124
5	at	SMU.1004	*gtfB*	glucosyltransferase	NC_004350	953133
6	ag	SMU.1004	*gtfB*	glucosyltransferase	NC_004350	953144
7	tc	SMU.1004	*gtfB*	glucosyltransferase	NC_004350	953145
8	at	SMU.1004	*gtfB*	glucosyltransferase	NC_004350	953151
9	ta	SMU.1004	*gtfB*	glucosyltransferase	NC_004350	953153
10	tg	SMU.1004	*gtfB*	glucosyltransferase	NC_004350	953154
11	tg	SMU.1004	*gtfB*	glucosyltransferase	NC_004350	953157
12	ag	SMU.1004	*gtfB*	glucosyltransferase	NC_004350	953158
13	cg	SMU.1004	*gtfB*	glucosyltransferase	NC_004350	953166
14	ct	SMU.1542c		lipid kinase	NC_004350	1471014
15	gc	SMU.1588c		hexosyltransferase	NC_004350	1518523
16	ac	SMU.1990c	*rpoB*	DNA-directed RNA polymerase subunit	NC_004350	1862650
17	ac	IGR SMU.2121c - SMU.2123		hypothetical protein	NC_004350	1990740
CTV3-7						
Number	SNP pattern	Gene	Name	Function	Location	
1	tC	SMU.25	*recO*	DNA repair protein	NC_004350	29442
2	tA	SMU.25 IGR		DNA repair protein - phosphate acyltransferase	NC_004350	29489
3	aT	SMU.25 IGR		DNA repair protein - phosphate acyltransferase	NC_004350	29540
4	aC	SMU.25 IGR		DNA repair protein - phosphate acyltransferase	NC_004350	29559
5	cA	SMU.25 IGR		DNA repair protein - phosphate acyltransferase	NC_004350	29598
6	aG	SMU.44		DNA mismatch repair	NC_004350	47444
7	aG	SMU.44		DNA mismatch repair	NC_004350	47530
8	aG	SMU.44 IGR		DNA mismatch repair - hypothetical protein	NC_004350	47892
9	gT	SMU.44 IGR		DNA mismatch repair - hypothetical protein	NC_004350	49100
10	aT	pyrG - fbaA IGR		fructose bisphosphate aldolase	NC_004350	100116
11	aT	SMU.112c		transcriptional regulator	NC_004350	112507
12	tA	purA - sgaT IGR		adenylosuccinate synthetase - PTS	NC_004350	261148
13	tA	purA - sgaT IGR		adenylosuccinate synthetase - PTS	NC_004350	261178
14	gC	SMU.502		hypothetical protein	NC_004350	470965
15	tC	SMU.504	*dam*	site-specific DNA methylase	NC_004350	474498
16	aG	SMU.515 - SMU.516 IGR		hypothetical protein(s)	NC_004350	484132
17	aG	SMU.562c - SMU.563 IGR	*clpE*	ATP-dependent protease	NC_004350	527485
18	tG	SMU.562c - SMU.563 IGR	*clpE*	ATP-dependent protease	NC_004350	527506
19	aC	SMU.562c - SMU.563 IGR	*clpE*	ATP-dependent protease	NC_004350	527563

20	cT	SMU.597	*pbp2b*	pencillin binding protein 2b	NC_004350	554999
21	tC	SMU.597	*pbp2b*	pencillin binding protein 2b	NC_004350	555170
22	aC	SMU.616		hypothetical protein	NC_004350	578092
23	aG	SMU.618 - SMU.620 IGR		hypothetical protein(s)	NC_004350	578744
24	cT	SMU.618 - SMU.620 IGR		hypothetical protein(s)	NC_004350	578748
25	tA	SMU.618 - SMU.620 IGR		hypothetical protein(s)	NC_004350	578750
26	aG	SMU.683		ATP-binding protein	NC_004350	648149
27	aT	SMU.758c - SMU.759 IGR		hypothetical protein - protease	NC_004350	710076
28	aT	SMU.758c - SMU.759 IGR		hypothetical protein - protease	NC_004350	710126
29	tA	SMU.773c - SMU.774 IGR		tRNA-synthetase - hypothetical protein	NC_004350	724043
30	gT	SMU.773c - SMU.774 IGR		tRNA-synthetase - hypothetical protein	NC_004350	724044
31	tC	SMU.773c - SMU.774 IGR		tRNA-synthetase - hypothetical protein	NC_004350	724046
32	aC	SMU.773c - SMU.774 IGR		tRNA-synthetase - hypothetical protein	NC_004350	724048
33	aG	SMU.773c - SMU.774 IGR		tRNA-synthetase - hypothetical protein	NC_004350	724049
34	aC	SMU.773c - SMU.774 IGR		tRNA-synthetase - hypothetical protein	NC_004350	724050
35	cA	SMU.773c - SMU.774 IGR		tRNA-synthetase - hypothetical protein	NC_004350	724053
36	tA	SMU.773c - SMU.774 IGR		tRNA-synthetase - hypothetical protein	NC_004350	724057
37	aG	SMU.773c - SMU.774 IGR		tRNA-synthetase - hypothetical protein	NC_004350	724059
38	gA	SMU.773c - SMU.774 IGR		tRNA-synthetase - hypothetical protein	NC_004350	724061
39	aT	SMU.773c - SMU.774 IGR		tRNA-synthetase - hypothetical protein	NC_004350	724094
40	aC	SMU.895		DNA-damage inducible protein	NC_004350	850090
41	tG	SMU.923 - SMU.924		Rcr peptides SNP?	NC_004350	878588
42	tC	SMU.992 - SMU.993 IGR		hypothetical protein - GTPase	NC_004350	939662
43	tC	topA - gld IGR		DNA topoisomerase - tRNA	NC_004350	949062
44	aC	SMU.1010c	*citC*	citrate ligase	NC_004350	965767
45	tA	SMU.1010c	*citC*	citrate ligase	NC_004350	965816
46	aT	SMU.1033 - SMU.1034c IGR		site-specific tyrosine recombinase	NC_004350	982851
47	cG	SMU.1197 IGR		hypothetical protein	NC_004350	1140398
48	gT	SMU.1469 - SMU.1470c IGR		hypothetical protein	NC_004350	1395952
49	tG	SMU.1469 - SMU.1470c IGR		hypothetical protein	NC_004350	1395963
50	aC	covR - glnQ IGR		response regulator - ABC transporter	NC_004350	1447027
51	aG	covR - glnQ IGR		response regulator - ABC transporter	NC_004350	1447078
52	gT	SMU.1542c		lipid kinase	NC_004350	1470494
53	tG	SMU.1576c		hypothetical protein	NC_004350	1503438
54	gT	SMU.1708	*trkA*	potassium transporter	NC_004350	1619470
55	aC	SMU.1848		hypothetical protein	NC_004350	1745705
56	aT	SMU.1895c - 1897 iGR		hypothetical protein - ABC transporter	NC_004350	1783686

CTV3-8

Number	SNP pattern	Gene	Name	Function	Location	
1	gA	SMU.43		site-specific DNA methyltransferase modification protein	NC_004350	46486
2	cT	SMU.369c - SMU.370 IGR		hypothetical protein - ABC transporter	NC_004350	352139
3	tA	SMU.470		hypothetical protein	NC_004350	439254
4	aT	SMU.773c - SMU.774 IGR		tRNA-synthetase - hypothetical protein	NC_004350	724145
5	tG	SMU.804		hypothetical protein	NC_004350	750816
6	tG	topA - gld IGR		DNA topoisomerase - tRNA	NC_004350	949107
7	cT	SMU.1542c		lipid kinase	NC_004350	1471014
8	gC	SMU.1588c		hexosyltransferase	NC_004350	1518523
9	aC	SMU.2121c - SMU.2123 IGR		hypothetical protein	NC_004350	1990740

CTV3-9

Number	SNP pattern	Gene	Name	Function	Location	
1	gT	SMU.750c		hypothetical protein	NC_004350	703503
2	cG	SMU.875c		transposase	NC_004350	826253
3	tC	SMU.1005	*gtfC*	glucosyltransferase	NC_004350	957858
4	cT	SMU.1005	*gtfC*	glucosyltransferase	NC_004350	957915

5	aG	SMU.1005	*gtfC*	glucosyltransferase	NC_004350	957924
6	gC	SMU.1134c		phosphate transporter	NC_004350	1076258
7	tA	SMU.1332c - SMU.1334c IGR		transposase – phosphopantetheinyl transferase	NC_004350	1255056
8	tC	SMU.1332c - SMU.1334c IGR		transposase - phosphopantetheinyl transferase	NC_004350	1255058
9	aT	SMU.1336c	*pksD*	hypothetical protein	NC_004350	1257526
10	tC	SMU.1407c		Transposase	NC_004350	1337500
11	cT	SMU.1542c		lipid kinase	NC_004350	1471014
12	tA	SMU.1966c - SMU.1967c IGR		periplasmic sugar binding protein - ssb2	NC_004350	1843377
13	gT	SMU.1966c - SMU.1967c IGR		periplasmic sugar binding protein - ssb2	NC_004350	1843380
14	aC	SMU.2121c - SMU.2123 IGR		hypothetical protein	NC_004350	1990740
15	aC	SMU.2163	*htrA*	serine protease	NC_004350	2030550

CTV3-10						
Number	SNP pattern	Gene	Name	Function	Location	
1	cT	SMU.895		DNA-damage-inducible protein	NC_004350	850077
2	gA	SMU.1188c	*lepB*	signal peptidase	NC_004350	1129851
3	aT	SMU.1188c	*lepB*	signal peptidase	NC_004350	1129852
4	gT	SMU.1188c	*lepB*	signal peptidase	NC_004350	1129856
5	tC	SMU.1188c	*lepB*	signal peptidase	NC_004350	1129860
6	aT	SMU.1188c	*lepB*	signal peptidase	NC_004350	1129868
7	gA	SMU.1188c	*lepB*	signal peptidase	NC_004350	1129870
8	tC	SMU.1337c		alpha/beta hydrolase	NC_004350	1258225
9	gT	SMU.1542c		lipid kinase	NC_004350	1470494
10	cT	SMU.1588c		hexosyltransferase	NC_004350	1518644
11	cT	SMU.1773c		hypothetical protein	NC_004350	1677179

Table S2. Strains Used in This Study.

Strain	Respective Characteristics*	Reference
***S. mutans* strains**		
UA159	Wild-type	ATCC 700610
CTV3-1	Third-generation CHX passaged variant	This study
CTV3-3	Third-generation CHX passaged variant	This study
CTV3-6	Third-generation CHX passaged variant	This study
CTV3-7	Third-generation CHX passaged variant	This study
CTV3-8	Third-generation CHX passaged variant	This study
CTV3-9	Third-generation CHX passaged variant	This study
CTV3-10	Third-generation CHX passaged variant	This study
Δ804	Non-polar Km marker replacement of SMU.804; Km^R	This study
Δ1576c	Non-polar Km marker replacement of SMU.1576c; Km^R	This study
***S. gordonii* strains**		
DL1	Wild-type	ATCC 35105
***S. sanguinis* strains**		
SK150	Wild-type	Lab Stock
***S. australis*-like strains**		
A12	Wild-type	Lab Stock

* Km, Kanamycin

Table S3. Primers Used in This Study.

Primer Name	Sequence (5' -> 3')*	Use
16S-F	AGA GTT TGA TCC TGG CTC AG	16S rRNA Sequencing of CTV3s
16S-R	TAC GGG TAC CTT GTT ACG ACT	16S rRNA Sequencing of CTV3s
804-F	CCT GTG GTT TGT CGC CTA GTC TC	Forward Amplification of SMU.804 for Sequencing
804-R	GCC ACT ATT GTG GAC TGA CTT GCA C	Reverse Amplification of SMU.804 for Sequencing
804-Seq1	GTT TTT CAA TGC ACC TTA CCT CC	Nested Sequencing Primer 1 of SMU.804
804-Seq2	ACA AGG ATG TGA TTA TTC CGA AG	Nested Sequencing Primer 2 of SMU.804
804-Seq3	GAG GAG AAT AAG ATA GAT ATT TCA GG	Nested Sequencing Primer 3 of SMU.804
804-Seq4	GTT TAG CAA CAC TGT TAT TGC	Nested Sequencing Primer 4 of SMU.804
804-A	CGT CGT CAA ATC GCT GAC TGT C	PCR for Arm 1 in Construction of △804
804-B	CAT GGG ATC CTG ACT TTT TGA AAG CG	PCR for Arm 1 in Construction of △804
804-C	GAG GGA TCC TTC ATT CTC AGT TCC GAC	PCR for Arm 2 in Construction of △804
804-D	GGA AGA AGC ACA AAA GCA TGG CAT GG	PCR for Arm 2 in Construction of △804
1542c-F	GTC TTG GTG CTA ATG TAG CTG G	Forward Amplification of SMU.1542c for Sequencing
1542c-R	CTG TCC GCT CTG CCA TTG C	Reverse Amplification of SMU.1542c for Sequencing
1542c-Seq1	AAC CAG TCT GGT CAT AGC GG	Nested Sequencing Primer 1 of SMU.1542c
1542c-Seq2	GAA GCT GCA CGT GCC AGT CAA GC	Nested Sequencing Primer 2 of SMU.1542c
1542c-Seq3	TCA TAT GGA TAT TGG TAG GGC	Nested Sequencing Primer 3 of SMU.1542c
1542c-Seq4	GGA GGC TTT GAA ACG ATT GC	Nested Sequencing Primer 4 of SMU.1542c
1576c-F	CAT TTG ATA TAG ATC CAA ATG ATG AGG	Forward Amplification of SMU.1576c for Sequencing
1576c-R	CAA GTG AAG GAA TTT CAA TCT CAT C	Reverse Amplification of SMU.1576c for Sequencing
1576c-A	CGA AAT TTT AGA AGT TTT GGA TCA GG	PCR for Arm 1 in Construction of △1576c
1576c-B	CTA TTT GGA TCC CCA TAT ATT AAA TCT CC	PCR for Arm 1 in Construction of △1576c
1576c-C	GTA GGA TCC AGT CTT AAA AAT TGA AGG G	PCR for Arm 2 in Construction of △1576c
1576c-D	CAT TAG CTG TAG CAA GTC CAT TGG	PCR for Arm 2 in Construction of △1576c
1588c-F	GGC TGG ATA ACT GAT GAA GCA G	Forward Amplification of SMU.1588c for Sequencing
1588c-R	GGC CTG CAC TTT CTC AGC TGC C	Reverse Amplification of SMU.1588c for Sequencing
1588c-Seq1	AGA GGC AGG TTA TTT AGT CGC CC	Nested Sequencing Primer 1 of SMU.1588c
1588c-Seq2	CGC AGA CAG AAT TTA GTC TGG G	Nested Sequencing Primer 2 of SMU.1588c
1588c-Seq3	GAC ATT AGT CAA GAA GAT ATT GCC	Nested Sequencing Primer 3 of SMU.1588c
1588c-Seq4	GCC GAT TAT CGC TCA GTC CAA TCC	Nested Sequencing Primer 4 of SMU.1588c

*Underlines represent BamHI Restriction Sites used in cloning

Table S4. NCBI SRA Accession Numbers.

Accession	Sample Name	SPUID	Organism	Tax ID	Strain	CTV3 isolate
SAMN10743465	JK1	JK1	Streptococcus mutans	1309	UA159	1
SAMN10743467	JK3	JK3	Streptococcus mutans	1309	UA159	3
SAMN10743470	JK6	JK6	Streptococcus mutans	1309	UA159	6
SAMN10743471	JK7	JK7	Streptococcus mutans	1309	UA159	7
SAMN10743472	JK8	JK8	Streptococcus mutans	1309	UA159	8
SAMN10743473	JK9	JK9	Streptococcus mutans	1309	UA159	9
SAMN10743474	JK10	JK10	Streptococcus mutans	1309	UA159	10
SAMN10743475	JKW	JKW	Streptococcus mutans	1309	UA159	parental

Figure S1

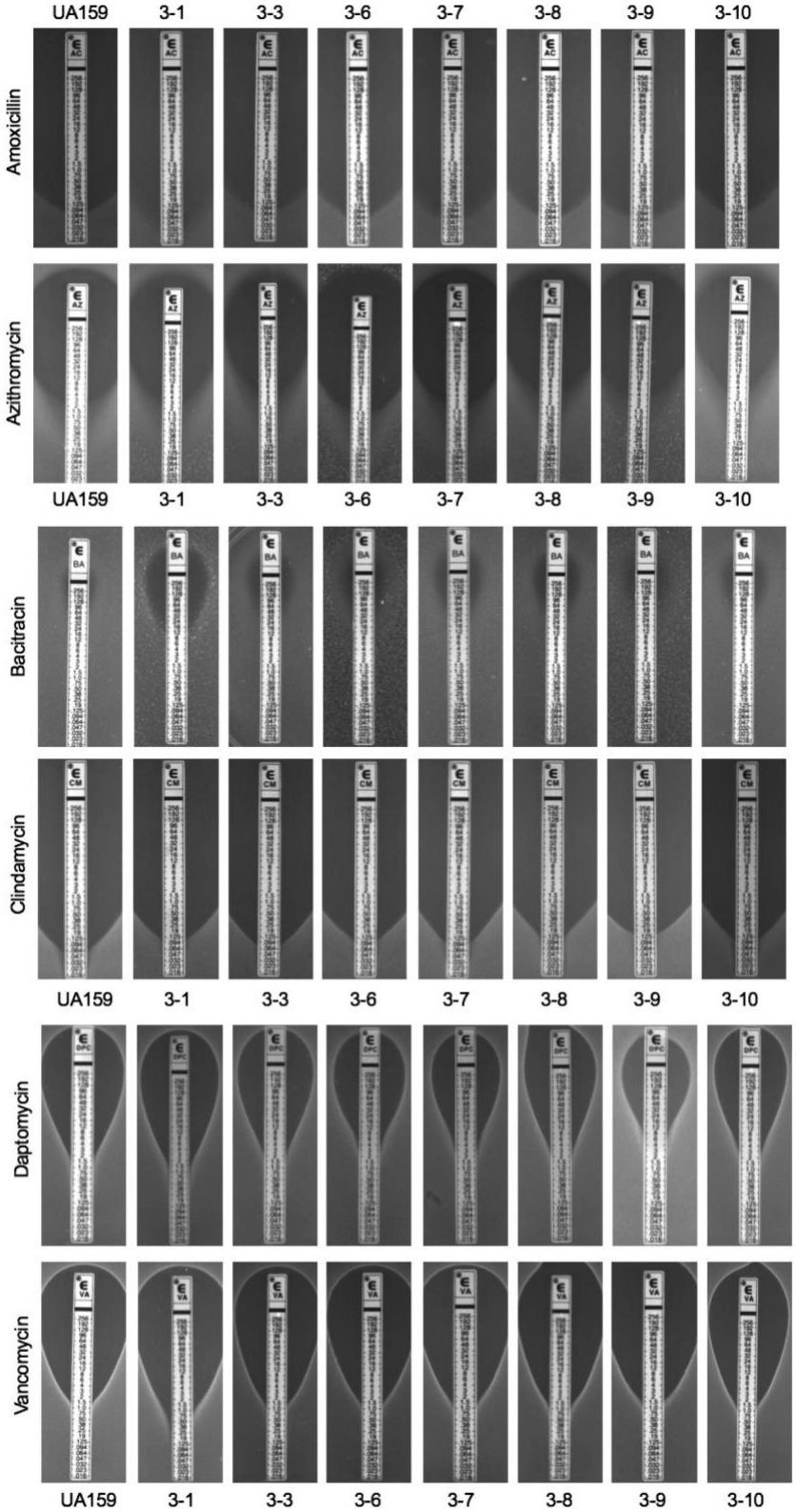

Supplemental Figure 1. Results of MIC Testing Using ETest Strips. To determine the MIC of various antibiotics using different mechanisms of action on the parental UA159 and CTV3s, 10 µL from a mid-exponential culture of the respective strain was added to 10 mL soft BHI agar (0.75% agarose) and overlaid on to BHI agar plates. Once solidified, ETEST strips (bioMérieux, Inc., Durham, N.C.) containing either Amoxicillin, Azithromycin, Bacitracin, Clindamycin, Daptomycin or Vancomycin when then laid over the agar with sterile forceps. After 48 h of growth at 37°C in a 5% CO_2 aerobic atmosphere, the agar plates were examined, imaged and lowest MIC recorded where no growth was visible. Each image above is one representative image from three independent biological replicates tested.

Figure S2

```
S. aureus     ---MRKRARIIYNPTSGKEQFKRELPDALIKLEKAGYETSAYATEKIGD-ATLEAERAMH  56
S. mutans     MVRKQKRARLIYNPTSGQEIMKKNVAEVLDILESFGYETSAFQTTPRADSAKNEAARASQ  60
                  :****:*******:* :*::: :.*  **. ******: *   .* *. ** ** :

S. aureus     ENYDVLIAAGGDGTLNEVVNGIAEKPNRPKLGVIPMGTVNDFGRALHIPNDIMGA-LDVI  115
S. mutans     AGFDLVIAAGGDGTINEVVSGIAPLKRRPKVAIIPTGTTNDFARALKIPRGNPVEATKLI  120
               .:*::********:****.***   .***:.:** **.***.***:**..      .:*

                         G131S                           G164D
S. aureus     IEGHSTKVDIGK-MNNRYFINLAAGGQLTQVSYETPSKLKSIVGPFAYYIKGFEMLPQMK  174
S. mutans     GKNQTIHMDIGRAYNDKYFINIAAAGSLTELTYSVPSQLKTMFGYLAYLVKGAELLPRVR  180
               :.:: ::***:  *::****:**.*.**:::*..**:**::.* :** :** *:**:::

S. aureus     AVDLRIEYDGNVFQGEALLFFLGLTNSMAGFEKLVPDAKLDDGYFTLIIVEKSNLAELGH  234
S. mutans     NVPVKVFYDHGVFEGEASMIFVALTNSVGGFETIAPDAKLDDGKFTLILVKTANLFELTD  240
               * ::: ** .**:*** ::*:.****:.***.:.******** ****:*:.:** ** .

                       G249E
S. aureus     IMTLAS-RGEHTKHPKVIYEKAKAINIS----SFTDLQLNVDGEYGGKLPANFLNLERHI  289
S. mutans     LIRLVLTGGRHINHKKIEYIKTSYLKIIPQGNPPKRMMINLDGEYGGDAPIELRNLKNHI  300
              :: *.   *.* :* *: * *:. ::*       . : :*:******. * :: **:.**

                 A304D
S. aureus     DVFAPNDIVNEELINNDHVDDNLIE-------E--------------               315
S. mutans     EFFANTDEISDDAITLDTEELVLEAIAQKFAREAESLDEMDKTKEQD               347
              :.** .* :.:: *. *  :  *         *
```

Supplemental Figure 2. Alignment of DgkB. Alignment of the DgkB protein coding sequence between *Staphylococcus aureus* and *Streptococcus mutans* (1542c). Bolded red amino acids in the *S. mutans* sequence signify those residues that are mutated in the CTV3 variants, with the corresponding amino acid substitution found above. Sequences were aligned using the web tool Clustal Omega (https://www.ebi.ac.uk/Tools/msa/clustalo/).

786 **Figure S3**

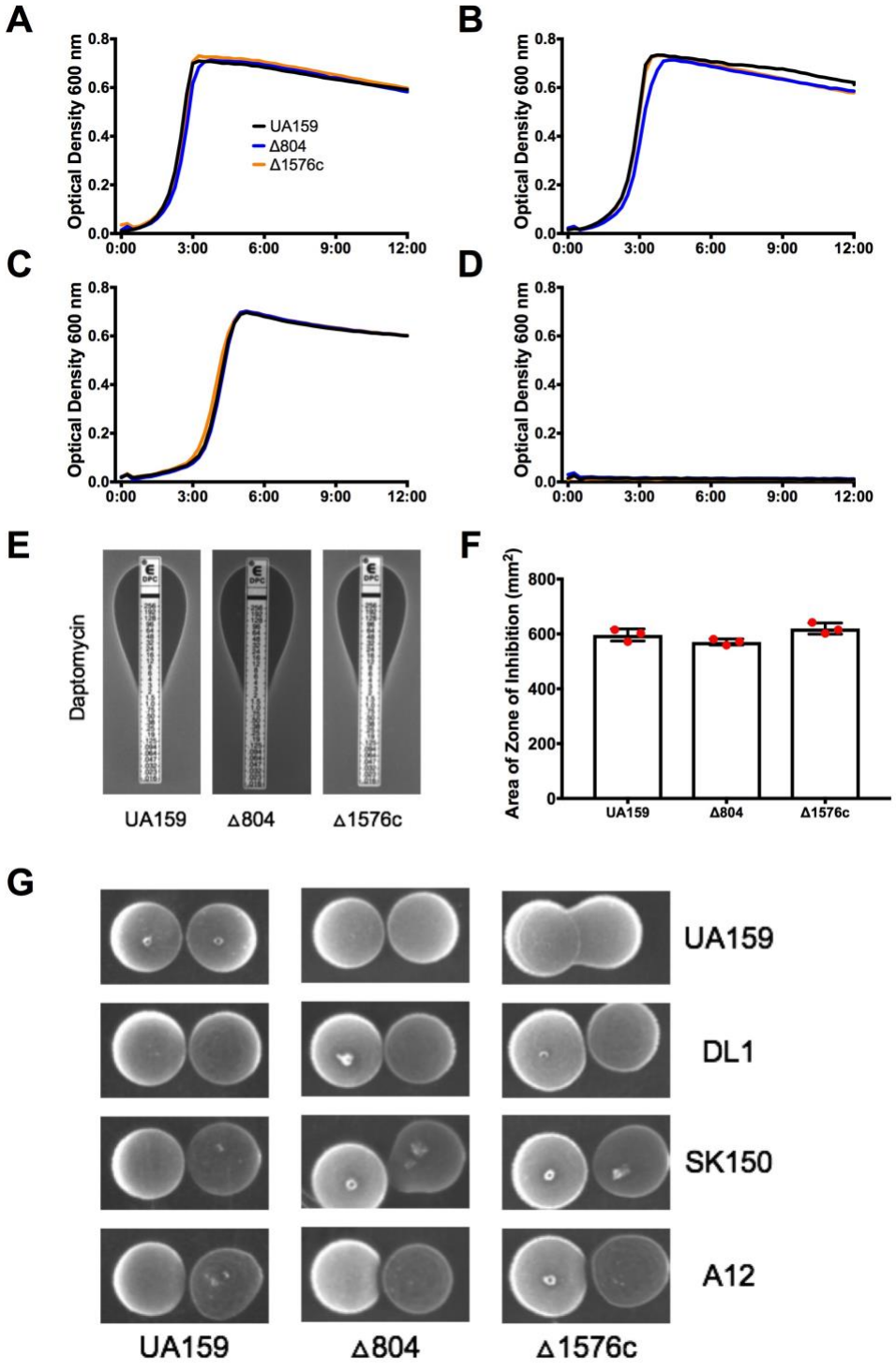

Supplemental Figure 3. Assaying of Δ804 and Δ1576c Phenotypes. Non-polar kanamycin antibiotic marker replacement mutants of Δ804 and Δ1576c were compared to the parental UA159 strain for the following phenotypes: (A) growth in BHI, (B) growth in BHI with 0.50 μg mL $^{-1}$ CHX, (C) growth in BHI with 0.75 μg mL $^{-1}$ CHX, (D) growth in BHI with 1.00 μg mL $^{-1}$ CHX, (E) ETEST Strip Assay with Daptomycin, (F) bacteriocin overlay assay with *S. sanguinis* SK150 as the indicator strain, and (G) plate-based antagonism assay.